

AIRE1A might be involved in cyclin B2 degradation in testicular lysates

M. Brahmaraju, K.P. Bhagya, Shiny Titus, Arun Sebastian, A.N. Devi, Malini Laloraya, and Pradeep G. Kumar

Abstract: The autoimmune regulator gene *Aire* shows predominant expression in thymus and other immunologically relevant tissues, and is assigned the major function of programming autoreactive T-cell deletion. However, the expression of this gene in tissues outside the immune system raises a question about its possible function beyond the T-cell deletion dogma. We detected *Aire* in mouse testis, and the expression of AIRE protein was remarkably high in postmeiotic germ cells. Sequencing results indicate that testis expressed *Aire* variant 1a. AIRE could be detected in spermatozoa, with heavy localization on the principal acrosomal domains. Mouse oocytes stained negatively for AIRE before fertilization, but stained positively for AIRE 30 min after fertilization. In the zygote, the levels of AIRE correlated negatively with cyclin B2 levels. Goat testicular lysates spiked with recombinant human AIRE exhibited augmented cyclin B2 degradation in the presence of protease inhibitors, which was inhibited by MG-132, indicating the operation of proteasomal pathways. Thus, this study identifies a correlation between the presence of AIRE and proteasomal breakdown of cyclin B2, which leads us to speculate that cyclin B2 could be a target of AIRE's E3-ubiquitin ligase activity.

Key words: autoimmune regulator, cyclin B2, fertilization, spermatozoa, testis, ubiquitin ligase.

Résumé : Le gène AIRE (*autoimmune regulator*) est exprimé de façon prédominante dans le thymus et d'autres tissus immunologiquement pertinents, et on lui attribue une fonction importante dans la programmation de la délétion des cellules T autoréactives. Cependant, l'expression de ce gène dans les tissus hors du système immunitaire soulève une question quant à sa fonction possible au-delà du dogme de la délétion des cellules T. Nous avons détecté *Aire* dans les testicules de souris, et l'expression d'AIRE est remarquablement élevée dans les cellules germinales supérieures post-méiotiques chez la souris. Les résultats de séquençage indiquent que les testicules expriment le variant *Aire* 1a. AIRE a pu être détectée dans les spermatozoïdes, avec une forte localisation dans les domaines acrosomiaux principaux. Les ovocytes de souris étaient négatifs à AIRE avant la fertilisation, mais étaient positifs 30 minutes après la fertilisation. Chez le zygote, les niveaux d'AIRE étaient négativement corrélés avec les niveaux de cycline B2. Des lysats testiculaires de bouc contenant de l'AIRE recombinante humaine dégradaient de façon accrue la cycline B2 en présence d'inhibiteurs de protéases, phénomène inhibé par le MG-132, indiquant que l'implication des voies de dégradation via le protéasome. Ainsi, cette étude a permis d'identifier une corrélation entre la présence de AIRE et la dégradation via le protéasome de la cycline B2, ce qui nous conduit à spéculer que la cycline B2 soit une cible de l'activité E3-ubiquitine ligase de AIRE.

Mots-clés : régulateur de l'autoimmunité, cycline B2, fertilisation, spermatozoïdes, testicules, ubiquitine ligase.

[Traduit par la Rédaction]

Introduction

The autoimmune regulator gene *Aire* encodes a multidomain protein containing CARD (caspase recruitment domain; Ferguson et al. 2008), SAND (Sp100, AIRE-1, NucP41/75, DEAF-1), and two PHD (plant homeo domain) domains. *Aire* is expressed heavily in thymic medullary epithelial cells, lymph nodes, and fetal liver, and plays a crucial role in maintaining central tolerance (Anderson et al. 2002; Hubert et al. 2008; Mittaz et al. 1999). Mutations in AIRE protein result in impaired auto antigen expression in thymus, setting the stage for the onset of autoimmune diseases (Puissant 2004; Zuklys et al. 2000) collectively known as autoimmune polyendocrinopathy-

candidiasis-ectodermal dystrophy (APECED) (Nagamine et al. 1997). Though widely discussed as a transcriptional coactivator, AIRE has also been shown to interact with DNA (Kumar et al. 2001), DNA-specific kinases such as DNAPK (Liiv et al. 2008), transcriptional elongation machinery pTEFB (Oven et al. 2007), and unmethylated histone H3 (Ooi et al. 2007; Zhao et al. 2009). The PHD1 domain of AIRE enables this protein to function as a unique ubiquitin E3 ligase (Uchida et al. 2004)

Although our understanding of the role of AIRE in central tolerance is progressing steadily, its impact on nonthymic locales remains poorly understood. RT-PCR analyses revealed that *Aire* mRNA is expressed in lung, kidney, adrenal gland

Received 30 November 2010. Revision received 27 March 2011. Accepted 19 April 2011. Published at www.nrcresearchpress.com/bcb on 08 August 2011.

M. Brahmaraju, K.P. Bhagya, S. Titus, A. Sebastian, A.N. Devi, M. Laloraya, and P.G. Kumar. Division of Molecular Reproduction, Rajiv Gandhi Centre for Biotechnology, Thycaud PO, Poojappura, Trivandrum 695 014, Kerala, India.

Corresponding author: Pradeep G. Kumar (e-mail: kumarp@rgcb.res.in).

ovary, and mouse testis (Heino et al. 2000; Ruan et al. 1999), suggesting that it might also have function(s) outside the immune system (Halonen et al. 2001; Kumar et al. 2002). AIRE-deficient mice showed a reduction in the scheduled wave of germ cell apoptosis, which is necessary for normal mature spermatogenesis, and an increase in sporadic germ cell apoptosis in testis (Schaller et al. 2008). Homozygous *Aire*-deficient mice (both male and female) were grossly normal, but were fertile only when crossed with wild-type partners. Moreover, successful pregnancies in homozygous crossings were very rare (Kuroda et al. 2005), indicating the importance of AIRE in early oocyte activation and (or) embryo development. Both spermatogenic wave (Yu and Wu 2008) and oocyte-activation (Duesbery and Vande Woude 2002) are dependent on nonproteolytic (Mahaffey et al. 1995) and ubiquitin-proteasome-mediated (Peter et al. 2001) degradation of cyclin B2. Since testis was one organ in which the presence of AIRE mRNA was reported, we evaluated the expression of *Aire* in mouse testis and its possible function as an E3-ubiquitin ligase in processing cyclin B2 for proteasomal degradation.

Materials and methods

Antibodies

Cyclin B2 and β -actin (rabbit polyclonal antibodies) were from Santa Cruz, California. Goat anti-rabbit horseradish peroxidase and goat anti-rabbit FITC were from Bangalore Genie, India. Anti-AIRE antibody was raised in rabbit against recombinant full-length human AIRE protein, as described in the Supplementary data.¹

Animals

Immature (1–2 weeks) and adult (3–5 months) male mice (*Mus musculus*, Swiss albino), bred and housed in the small animal facility of the institute were used for experiments. One adult male rabbit (a 1-year-old New Zealand white) was used for immunization experiments. The care and use of the animals, as well as the procedures performed on them were approved by the institutional animal ethical committee of Rajiv Gandhi Centre for Biotechnology, Trivandrum, India.

Microscopy

Fluorescence images were either visualized with a Nikon epifluorescence microscope or acquired using Leica SP2 AOBs confocal laser scan microscope. Photographs were taken with a Nikon Micro flex UFXII system.

RT–PCR and direct sequencing

mRNA from mouse testis was extracted using a Quick-Prep mRNA purification kit (GE Health Care, USA) and the concentration was adjusted to 50 μ g/mL. mRNA (2 μ g) was reverse-transcribed using a Ready-To-Go T-primed first strand synthesis kit (GE Health Care). PCR of the first strand was performed using the *Aire* gene-specific forward primer 5'-CAGCCCCTGTGAGGAAGAT-3' (–17F) and reverse primer 5'-CTGAGTCCAGCAGGCCA-GAAC-3' (1797R). The bands were eluted from the gel using an agarose gel purification kit (Qiagen, CA), and the

eluted DNA was subjected to dye termination chemistry using a BigDye sequencing kit (version 3.0; Applied Biosystems, USA). Dye-terminated products were analyzed using an ABI 3700 automated DNA sequencer. The experiment was repeated 5 times, and a consensus sequence was generated using Genedoc, version 3.0 (www.nrbsc.org/gfx/genedoc).

ClustalW multiple sequence alignment

The mouse testis *Aire* sequence was aligned with all the known transcript variants of *Aire* (NM_009646, AF079536, AF128115, AF128116, AF128117, AF128118, AF128119, AF128120, AF128121, AF128122, AF128123, AF128124, and AF128125). The output file was uploaded into Genedoc, version 3.0 (www.nrbsc.org/gfx/genedoc), and a shaded alignment file was generated.

Sperm preparation

Spermatozoa from testis and caput, corpus, and cauda epididymides of sexually mature male mice were recovered (Kumar et al. 1991). The sperm pellets were reconstituted in Krebs ringer bicarbonate (KRB) buffer to induce capacitation.

Capacitation and acrosome reaction of mouse spermatozoa

The spermatozoa (1×10^6 cells/mL) were placed in paraffin oil, incubated in plastic culture dishes for 2 h at 37 °C in KRB containing sodium pyruvate and sodium lactate in a 5% CO₂ incubator, and allowed to capacitate (Kumar et al. 1990). A crosome reaction was initiated by adding 3.18 μ mol/L progesterone dissolved in 0.05% dimethyl sulfoxide into the suspension of capacitated spermatozoa. The experiment was repeated five times and the means \pm SD were computed.

Sperm agglutination assay

Spermatozoa from the cauda epididymidis of adult mice were suspended in HBSS and incubated in the presence of anti-AIRE antibody that had been diluted 1:1000, 1:100, or 1:10. A control incubation was performed with rabbit preimmune serum that had also been diluted 1:1000, 1:100, or 1:10. The incubation was performed for 15 min in a 5% CO₂ incubator maintained at 37 °C.

Sperm-zona and sperm oolemma binding assay

Anti-AIRE antibodies (diluted 1:200 or 1:50) were added to the capacitation suspensions 2 h after the start of incubation. The control wells received equal dilutions of normal rabbit serum diluted 1:200 or 1:50, and the incubations were allowed to continue at 37 °C for 1 h.

A sterile 24-well tissue culture plate was maintained at 37 °C with 1 mL of KRB buffer. Ova collected from superovulated mice (Mizoguchi and Dukelow 1980) with and without zona pellucida were distributed in such a way that each well received 5–10 ova. The in vitro capacitated spermatozoa (200 μ L each) was added to the ova suspension and the plate was left undisturbed for 15 min. Ova with attached spermatozoa were transferred into fresh wells to release any

¹Supplementary data are available with the article through the journal Web site (www.nrcresearchpress.com/bcb)

unbound or loosely bound spermatozoa. The number of spermatozoa attached to each ovum at one focal plane was computed from a video projection of the oocyte by three different observers who were blinded to the experimental setup.

Oocytes fertilized in vitro

Unfertilized eggs collected from regularly cycling females were inseminated with 200 μ L of spermatozoa capacitated in vitro. Control oocytes were prepared by adding 200 μ L of KRB for mock insemination. After incubation with or without spermatozoa for 30 min, the oocytes were placed on concave slides.

Oocytes fertilized in vivo

Virgin female (Swiss strain) mice exhibiting a regular estrous cycle were mated with fertile males of the same strain to induce pregnancy. The animals were sacrificed on the first day of pregnancy. The fallopian tube was excised, washed in KRB, and minced finely to collect the fertilized eggs. The presence of a second polar body in the oocyte confirmed fertilization, and such oocytes were considered to be zygotes.

Protein extraction and Western blotting

Testis, thymus, bone marrow, and salivary glands were recovered from sexually mature male mice. The tissues and sedimented spermatozoa, prepared as described above, were placed in homogenization vials containing 0.5 mL solubilization buffer (187 mmol/L Tris-HCl, pH 6.8; 2% SDS; 0.05% 3-[(3-cholamidopropyl) dimethylammonio]-1-propanesulfonate (CHAPS); 10% glycerol; 1 mmol/L phenylmethylsulfonyl fluoride (PMSF); 1 mmol/L ethylene glycol tetra acetic acid (EGTA); and 1 mmol/L sodium orthovanadate) and were sonicated for 3 cycles of 10 s each at a 15 μ m amplitude (Soniprep 150, MSE, USA). The samples were centrifuged at 14 000g for 5 min and the supernatants were saved. Protein concentrations were determined using a DC Protein Assay kit (Bio-Rad, California) and adjusted to 20 μ g protein/10 μ L.

The denatured samples (30 μ g protein/well), resolved by 12% SDS-PAGE, were electro-blotted onto a PVDF membrane (0.2 μ m; BioRad, Hercules, California; Kumar et al. 2001). The membranes were incubated for 2 h in 5% non-fat milk in Tris-buffered saline containing 0.1% Tween 20, followed by a 1-h incubation with 1:10000 dilutions of the primary antibodies and a 1:5000 dilution of anti-rabbit IgG-peroxidase at room temperature. The blots were washed extensively and developed using a standard diaminobenzidine colour reaction. Western blots were subjected to quantitative analysis using Advanced Phoretix 1.0 (Nonlinear Dynamics, California) and the results were averaged. All observations were subjected to a one-way analysis of variance using Sigmaplot 4.0 (SPSS, California).

Immunoprecipitation and peptide mass fingerprinting

Testicular lysate (1 mL) with a protein concentration of 1 mg/mL was incubated with 10 μ g antiAIRE antibody for 1 h at 27 °C, followed by an overnight incubation at 4 °C with constant shaking. The reaction was incubated with 10 μ g protein A agarose for 1 h at 27 °C. The immunocomplex was precipitated by centrifugation at 14 000g for 30 min at 4 °C. The recovered pellet was washed by resuspension in

2 mL PBS-T (10 mmol/L, pH 7.4) followed by centrifugation at 14 000g. This procedure was repeated 3 times and the final pellet was boiled for 5 min at 95 °C with Laemmli denaturing buffer. The supernatant was resolved by SDS-PAGE and the bands were visualized by staining with Coomassie brilliant blue R-250. Protein bands were excised and processed for in-gel digestion using a Trypsin Profile IGD kit (Sigma Chemical Company, USA), following the manufacturer's instructions. Excised bands were trimmed into small pieces, destained with 200 μ L destaining solution twice at 37 °C for 30 min in an eppendorf tube, and dried in a vacuum drier for 25 min. After drying, protein gel pieces were digested by an overnight incubation with 20 μ L trypsin (0.4 μ g final concentration) in trypsin reaction buffer (50 μ L) at 27 °C. Tryptic peptides were purified and concentrated using Zip Tip concentrator. The samples were applied to MALDI plates and were co-crystallized with α -cyanonaphthol. The samples were analyzed on a Kratos MALDI-ToF mass spectrometer (Shimadzu, Japan) operating in the reflectron mode. Peptide mass data were analyzed using Mascot software (www.matrixscience.com).

Immunohistochemistry

Testis recovered from immature and mature mice were fixed in 4% paraformaldehyde at 4 °C, embedded in paraffin wax, and sectioned. The tissue sections (6 μ m) were incubated with blocking solution (5% normal goat serum) for 2 h. The tissue sections were then incubated overnight with anti-AIRE antibody (diluted 1:200), incubated 1 h with secondary goat anti-rabbit antibody conjugated with FITC (diluted 1:200), and incubated for 30 min with propidium iodide (diluted 1:1000). The slides were washed with PBS, mounted, and imaged.

Immunocytochemistry

Spermatozoa collected from different stages were smeared onto lysine-coated glass slides, fixed in 4% paraformaldehyde for 10 min, and washed in PBS containing 1% Tween-20 (PBS-T). Oocytes and zygotes were neutralized in 0.5 mol/L ammonium chloride permeabilized with 0.25% Triton X-100 and chilled ethanol, and incubated in a blocking solution containing 1% gelatin in PBS-T. For sperm preparations, 2% non-fat dry milk in PBS-T was used as blocker. Following an overnight incubation at 4 °C in a 1:200 dilution of the corresponding antibody in blocking solution, the slides were incubated with 1:200 dilutions of FITC-conjugated goat anti-rabbit IgG in blocking solution. Observations were made on three replicates and the average of the total green channel signal per oocyte was computed from nine individual oocytes for each of the experiments.

Cyclin B2 degradation assay

Goat testicular protein was extracted in solubilization buffer and the protein concentration was adjusted to 10 μ g/ μ L. This extract was used as a source of cyclin B2 and ubiquitin. Recombinant AIRE expressed in *Escherichia coli* (BL21DE3) was purified on HisTrap™ Fast Flow columns (GE Healthcare Life Sciences, Pennsylvania) and reconstituted to 1 mg/mL. Bacterial cell lysate (1 mg/mL) from untransformed BL21DE3 was used as a source of various E1s and E2s (designated BL21 (DE3)-AIRE). The reaction to

test the ability of AIRE to degrade cyclin B2 contained 5 μ L goat testicular proteins, 2 μ L purified AIRE, 2 μ L BL21 (DE3)-AIRE, and 1 μ L PBS containing ATP (2 mmol/L), MgCl₂ (2 mmol/L), and ZnCl (0.1 mmol/L). The reaction was incubated for 2 h at 30 °C. In another reaction, 2 μ L cell lysate from *E. coli* expressing AIRE (designated BL21 (DE3)+AIRE) replaced purified AIRE or BL21(DE3)-AIRE, with all other reagents remaining unaltered. Control reactions received BL21 (DE3)-AIRE lysate, and AIRE was excluded from this reaction. MG-132 (5 μ mol/L; *N*-(benzyloxycarbonyl) leucyl leucyl leucinal) was added in assays in which the inhibition of proteasome activity was intended. Reactions were terminated by boiling at 95 °C in Laemmli buffer containing β -mercaptoethanol. Samples were resolved on a 12% gel and Western blotted with cyclin B2 antibody. This experiment was repeated five times and the results were averaged.

Results

Aire expression in the testis

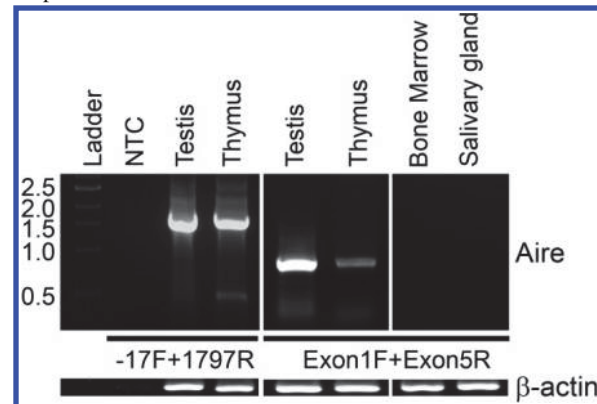
Using RT-PCR analysis employing *aire*-specific primer (–17 forward and 1797 reverse), we detected an amplification estimated to be 1.6 kb, which was comparable to the amplification obtained in mouse thymus cDNA used as a positive control (Fig. 1). Amplification using primers exon1F and exon5R, which would produce a 628-bp band from cDNA and a 1.9-kb band from genomic DNA, excluded the possibility of genomic DNA contamination in our reactions. cDNA prepared from bone marrow and salivary gland, which do not express *aire*, served as negative controls (Fig. 1). Direct sequencing of the 1.6 kb band obtained from testicular cDNA yielded full-length *aire* (GenBank accession No EU625343) that has been designated mouse testicular *aire* (*mtAire*). Multiple sequence alignment of *mtAire* with the known variants of mouse thymus *aire* transcripts (Fig. 2) indicated the absence of two deletions; i.e., a 12-bp deletion in the 794- to 805-bp region, and a 3-bp deletion in the 888- to 890-bp regions (both indicated with boxes in Fig. 2), as well as the presence of the 1102- to 1278-bp segment (indicated with a solid line in Fig. 2), confirmed that the mouse testis expresses *Aire* transcript variant 1a (*mtAire1a*).

Specificity of anti-AIRE antibody

Immunoprecipitated protein complex yielded three well resolved bands at molecular masses that were estimated to be 75, 62, and 55 kDa. Peptide mass fingerprinting of these bands identified these bands as Laminin B2 chain, autoimmune regulator, and immunoglobulin G heavy chain, respectively (Fig. 3A).

On Western blots, protein extracts from whole testis and thymus stained positively for AIRE, while bone marrow and salivary gland stained negatively. AIRE-positive bands in testis and thymus extracts could be abolished by the introduction of rAIRE at 1 μ g/mL (final concentration) in incubations with primary antibody, indicating the specificity of the antibody used. Protein extracts from spermatozoa from testis, various segments of epididymis, and vas deferens showed immunopositive bands with anti-AIRE antibody. Mouse thymus extract and recombinant AIRE were used as

Fig. 1. *Aire*-specific primers –17 forward (–17F) and 1797 reverse (1797R) produced a 1.5-kb product from testis and thymus cDNA. Amplification with primers exon1F and exon5R produced approximately 650-bp bands from testis and thymus cDNAs, and no amplification was seen from bone marrow or salivary gland cDNA. NTC, no template control.



a positive control and β -actin served as a loading control (Fig. 3B).

Immunohistochemical analysis of AIRE expression in testis

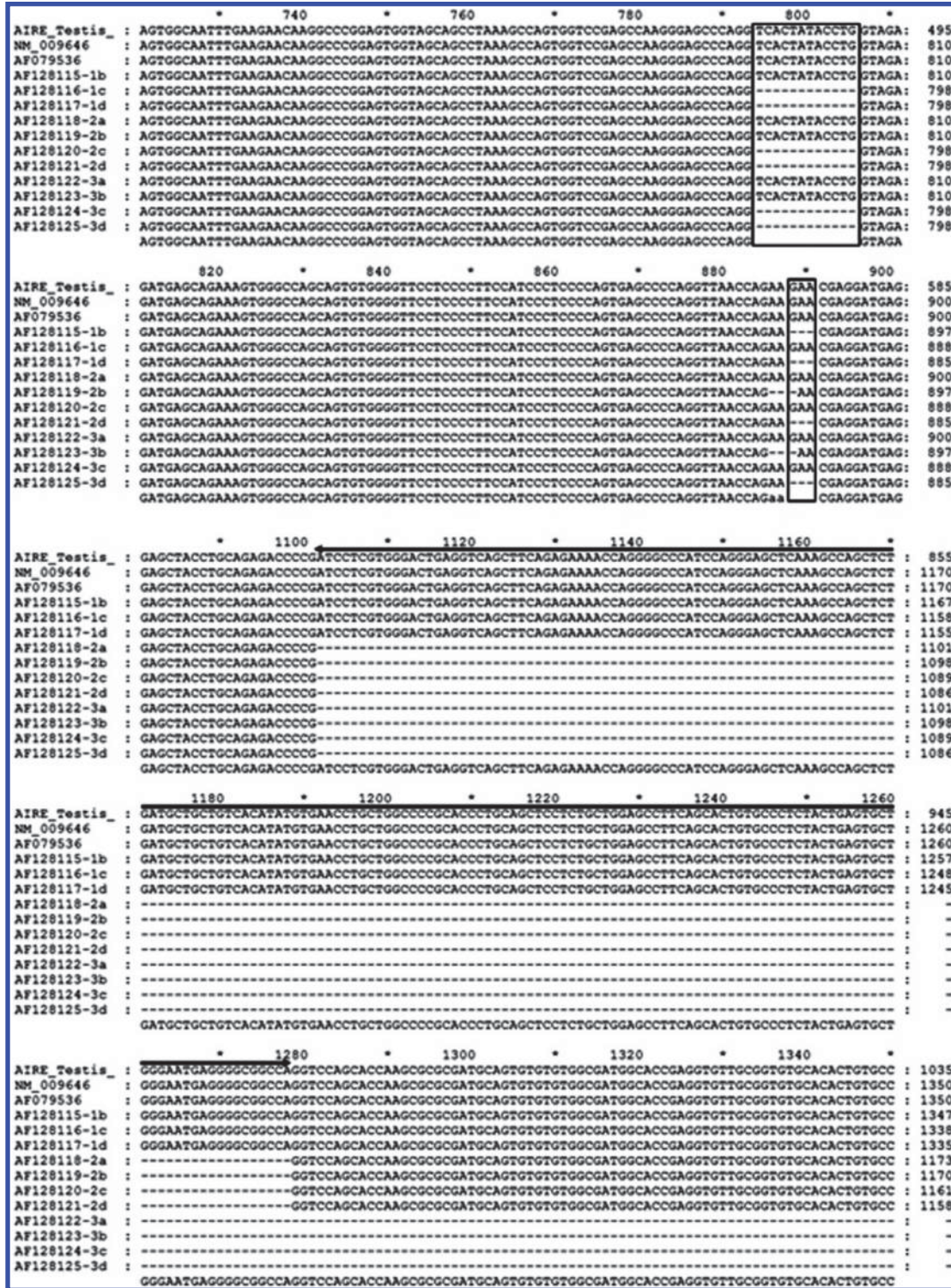
AIRE was localized in sections of mouse testis using immunohistochemistry followed by confocal laser scan microscopy. AIRE was characteristically localized in immature mouse testis in abundance in the spermatogonia located towards the basal side of the seminiferous tubules, and in moderate quantities in spermatogonia dispersed away from the basal epithelium (Fig. 4A). The nuclei were visualized under the red channel (Fig. 4B). Moreover, AIRE localization was predominantly nuclear in the spermatogonia of immature testis, as could be interpreted from the perfect overlay between the green (AIRE) and red (nucleus) channels in Fig. 4C. On the other hand, mature testis revealed moderate levels of the AIRE expression in spermatogonia and primary spermatocytes, whereas the cells located towards the luminal side, which are predominantly secondary spermatocytes and spermatids, stained strongly for AIRE (Fig. 4G). The nuclei were visualized under red channel (Fig. 4H) and the overlay was generated (Fig. 4I). Negative controls, in which the primary antibody was preblocked by incubating with 1 μ g/mL (final concentration) recombinant AIRE (Figs. 4D–4F and 4J–4L), showed near total loss of fluorescence in the green channel, indicating the specificity of the primary antibody used. A section of salivary gland was used as an AIRE-negative tissue to further validate the specificity of the antibody used (Figs. 4M–4O).

AIRE localization on the spermatozoa

Since the immunofluorescence studies on testis sections and Western blot analysis of sperm proteins indicated the presence of AIRE protein in spermatozoa, we conducted experiments to map the spatio-temporal distribution of AIRE on mouse spermatozoa recovered from various segments of the male reproductive tract.

AIRE was mostly localized to the head and mid-piece segments of the spermatozoa at all stages of development

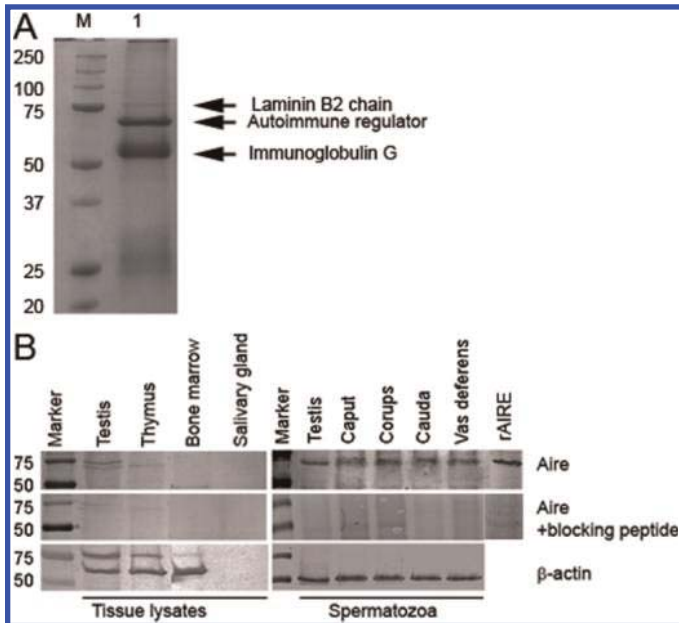
Fig. 2. ClustalW alignment of mouse testicular Aire with all the known transcript variants of Aire. NM_009646 and AF079536 (the longest Aire variants in mouse thymus) represent variant 1a, and the nucleotide numbering is based on the sequence of this variant. Other Aire variants (1b–1d and 2a–2d) are labeled. (A) Boxed areas highlight the deletions at 794–805 bp and 888–890 bp, which is typical in some variants. A third area (1102–1278 bp) which is present exclusively in Aire variant 1, is indicated with a solid line running above the sequence.



studied (Fig. 5). Testicular spermatozoa showed a weak and diffuse presence of AIRE on the equatorial domain and post-acrosomal domains (Fig. 5A). However, spermatozoa from epididymis showed a progressive trend of developing an

equatorial zone that was AIRE-negative (Figs. 5B–5D). At the same time, the postacrosomal domain of the spermatozoa from these regions showed an accumulation of AIRE (Figs. 5B–5D). Spermatozoa from vas deferens showed

Fig. 3. (A) Immunoprecipitation of proteins from mouse testis lysates, analyzed by mass spectroscopy. M, molecular mass marker; lane 1, immunoprecipitated proteins separated by SDS-PAGE. Arrows indicate the proteins and their identities. (B) Western blot analysis of AIRE expression in mouse tissues. Tissue lysates of adult testis, thymus, bone marrow, salivary gland, and lysates of spermatozoa harvested from testis, caput epididymidis, corpus epididymidis, cauda epididymidis, and vas deferens were evaluated for AIRE expression. Recombinant AIRE was used as a positive control and β -actin was used as loading control. Though salivary gland showed no β -actin band, the loading was confirmed by staining the gel with Coomassie Brilliant Blue (not presented).

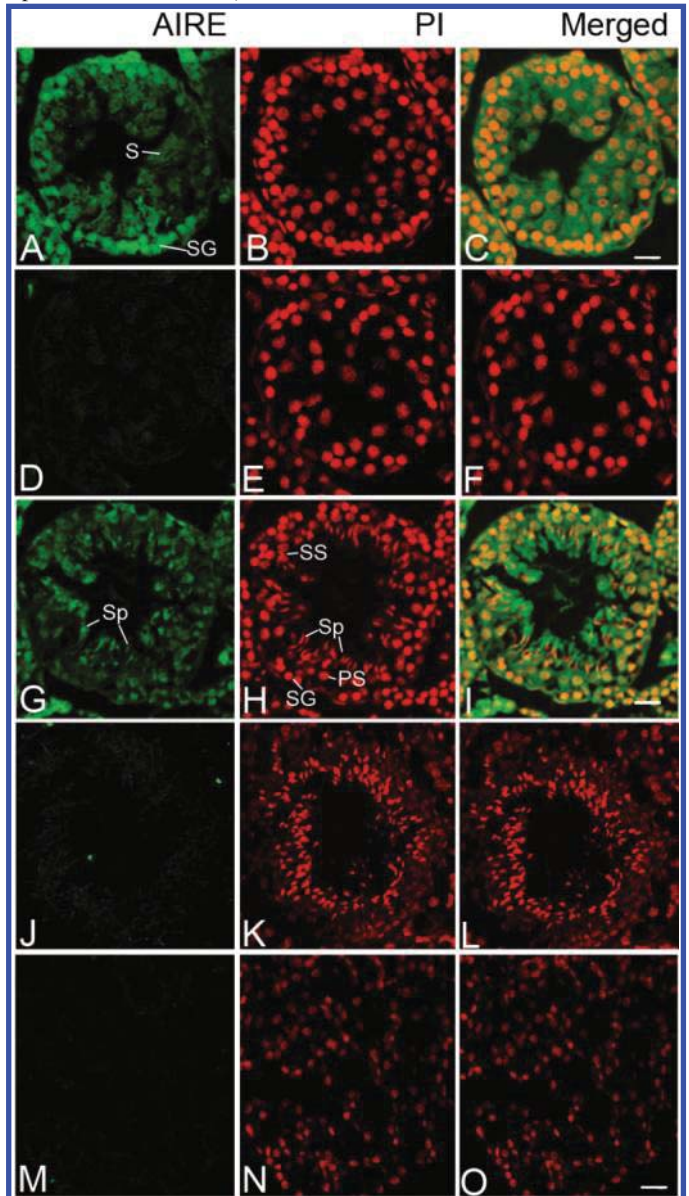


heavy localization of AIRE on the principal acrosomal domain and postacrosomal domains, with the equatorial domain showing moderate fluorescence. Strikingly, spermatozoa from this stage showed a very heavy localization of AIRE on their mid-piece as well (Fig. 5E). Capacitation *in vitro* brought about reorganization of AIRE exclusively onto the principal acrosomal domain (Fig. 5F). Progesterone-induced acrosome reaction in capacitated spermatozoa resulted in the loss of heavy fluorescence on the principal acrosomal domain, and the entire head and mid piece demonstrated a diffuse fluorescence (Fig. 5G). Negative controls prepared by preincubating the primary antibody with recombinant AIRE ($1\mu\text{g/mL}$, final concentration) abolished the staining described above (Figs. 5H–5N), indicating the specificity of the antibody used.

Sperm agglutination, sperm-zona interaction, and sperm oolemma binding assays

Spermatozoa were incubated with three different concentrations of anti-AIRE antibody to evaluate the accessibility of AIRE protein on sperm surfaces. The spermatozoa showed antibody-titer-dependent head-to-head agglutination patterns (Figs. 6B–6D), whereas preimmune serum did not induce spermatozoa agglutination (Fig. 6A). Furthermore, anti-AIRE antibody inhibited sperm-zona pellucida binding (Fig. 6F) and sperm-oolemma binding (Fig. 6, H), whereas preimmune serum had a negligible effect (Figs. 6E and 6G).

Fig. 4. Immunohistochemical localization of AIRE in immature and mature mouse testis. Sections of immature (A–C) and adult (G–I) testes were studied; corresponding controls (D–F and J–L) contained the primary antibody, which was pre-incubated with an excess of recombinant AIRE. AIRE localization is shown in the green channel, propidium iodide-staining is shown in the red channel, and the composite image is shown in the merged channel. The fluorescence patterns (A and G) could be abolished totally by incubating excess AIRE with primary antibody (D and J). Sections of salivary gland tissue probed with anti-AIRE antibody (M–O), served as the negative control. SG, spermatogonia; PS, primary spermatocyte; SS, secondary spermatocyte; Sp, spermatid; Se, Sertoli cell; S, spermatozoa. Bar = $5\mu\text{m}$.



AIRE localization in mouse oocytes and zygotes

Mouse oocytes collected from the oviduct after super ovulation (as described in Materials and methods) stained negatively for AIRE (Figs. 7A–7D). The oocytes were fertilized *in vitro* and the resulting zygotes exhibited heavy localization of AIRE both in the cytoplasm and the nucleus within 30 min of sperm entry (Figs. 7E–7H).

Fig. 5. AIRE protein distribution on mouse spermatozoa at various stages of development. Confocal fluorescence and bright field images of spermatozoa from testis (A), caput epididymids (B), corpus epididymidis (C), cauda epididymidis (D), vas deferens (E), capacitated in vitro (F), and acrosome reacted (G) are presented. The principal acrosomal domain is indicated with an arrow. H, head; M, mid-piece; T, tail. The fluorescence patterns (A–G) could be abolished by the incorporation of excess AIRE as a blocking protein in the incubation with primary antibody (H–N). Magnification, $\times 480$.

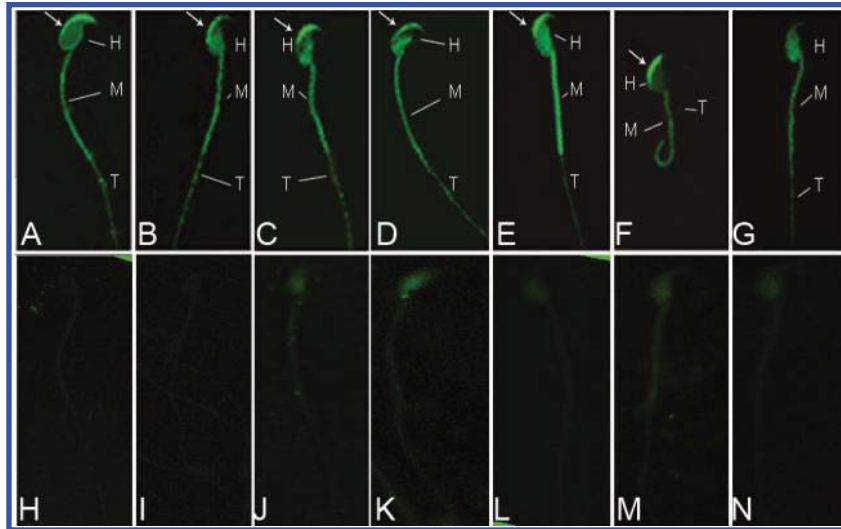


Fig. 6. The effect of anti-AIRE antibodies on sperm agglutination (A–D) and sperm–oocyte interaction (E–H). There was no detectable sperm agglutination in the presence of a 1:10 dilution of preimmune serum (A). Anti-AIRE antibodies at dilutions of 1:1000 (B), 1:100 (C), and 1:10 (D) dilutions brought about clearly visible agglutination in sperm suspensions, and are indicated with arrows. Sperm–zona pellucida interaction assays in the presence of a 1:10 dilution of preimmune serum (E) and a 1:50 dilution of anti-AIRE antibody (F). Sperm–olemma interaction assay in the presence of a 1:50 dilution of preimmune serum (G) and a 1:50 dilution of anti-AIRE antibody (H). Magnification, $\times 480$.

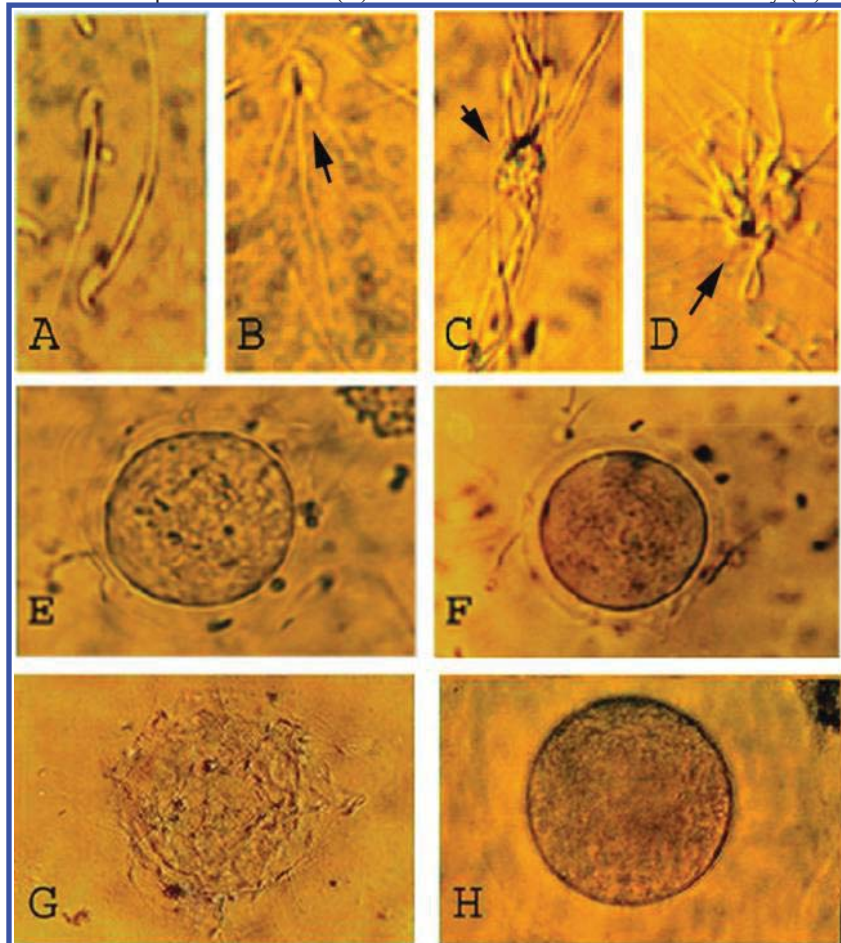
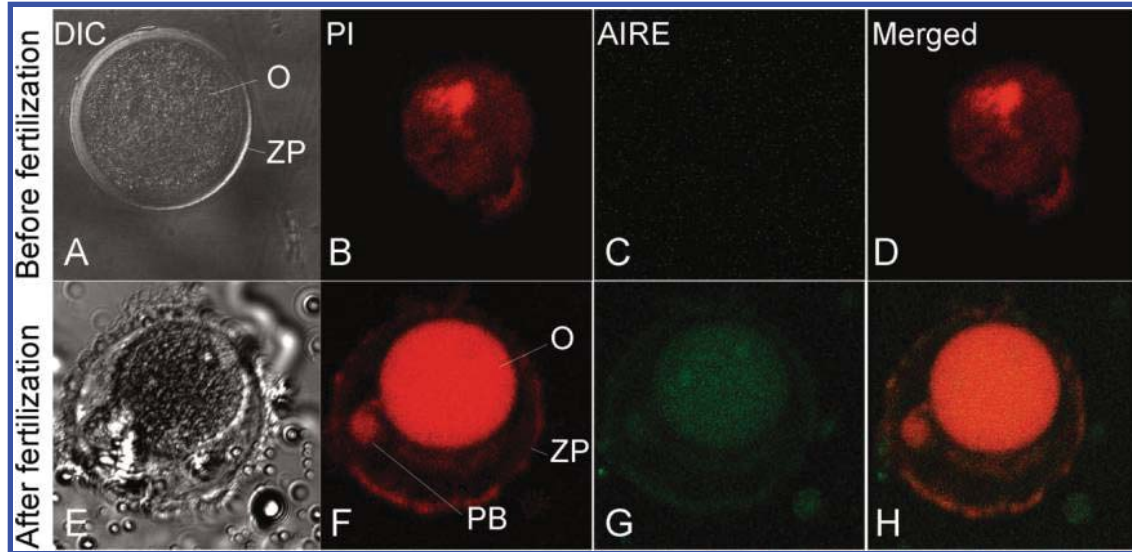


Fig. 7. Unfertilized oocytes before in vitro fertilization, as observed under differential interference contrast (A), stained with propidium iodide (B), and probed for AIRE (C). D is a merged image of B and C. An oocyte after in vitro fertilization observed under differential interference contrast (E) was imaged after staining with propidium iodide (F) and probing for AIRE (G). H is a merged image of F and G. O, oocyte; P, polar body; ZP, zona pellucida. Magnification, $\times 480$.



Experiments to evaluate the localization of AIRE in mouse oocytes before and after fertilization in vivo indicated that mouse oocytes were negative for AIRE before sperm entry (Figs. 8A–8D). Interestingly, we observed heavy localization of AIRE in the zygote cytoplasm (Figs. 8E–8H). Oocyte nucleus could be seen in the red (Figs. 8C and 8G) and in the merged channels (Figs. 8D and 8H).

Confocal microscopy analysis of the oocyte indicated heavy and diffused localization of cyclin B2 in the oocytes before sperm entry (Figs. 8J and 8L), and a quantitative reduction after fertilization (Figs. 8N and 8P). Ubiquitin showed a heavy localization in oocytes before (Figs. 8R and 8T) and after fertilization (Figs. 8V and 8X). The average green channel fluorescence per oocyte yielded quantitative information about the levels of AIRE, cyclin B2, and ubiquitin in the oocytes both before and after fertilization. Thus, after fertilization, AIRE levels rose very significantly from AIRE's near-zero levels in the oocyte before fertilization ($p < 0.001$). This observation correlated with a 2.5-fold decrease in the levels of cyclin B2 in the oocyte after fertilization ($p < 0.001$).

AIRE-dependent degradation of cyclin B2 in testicular lysates

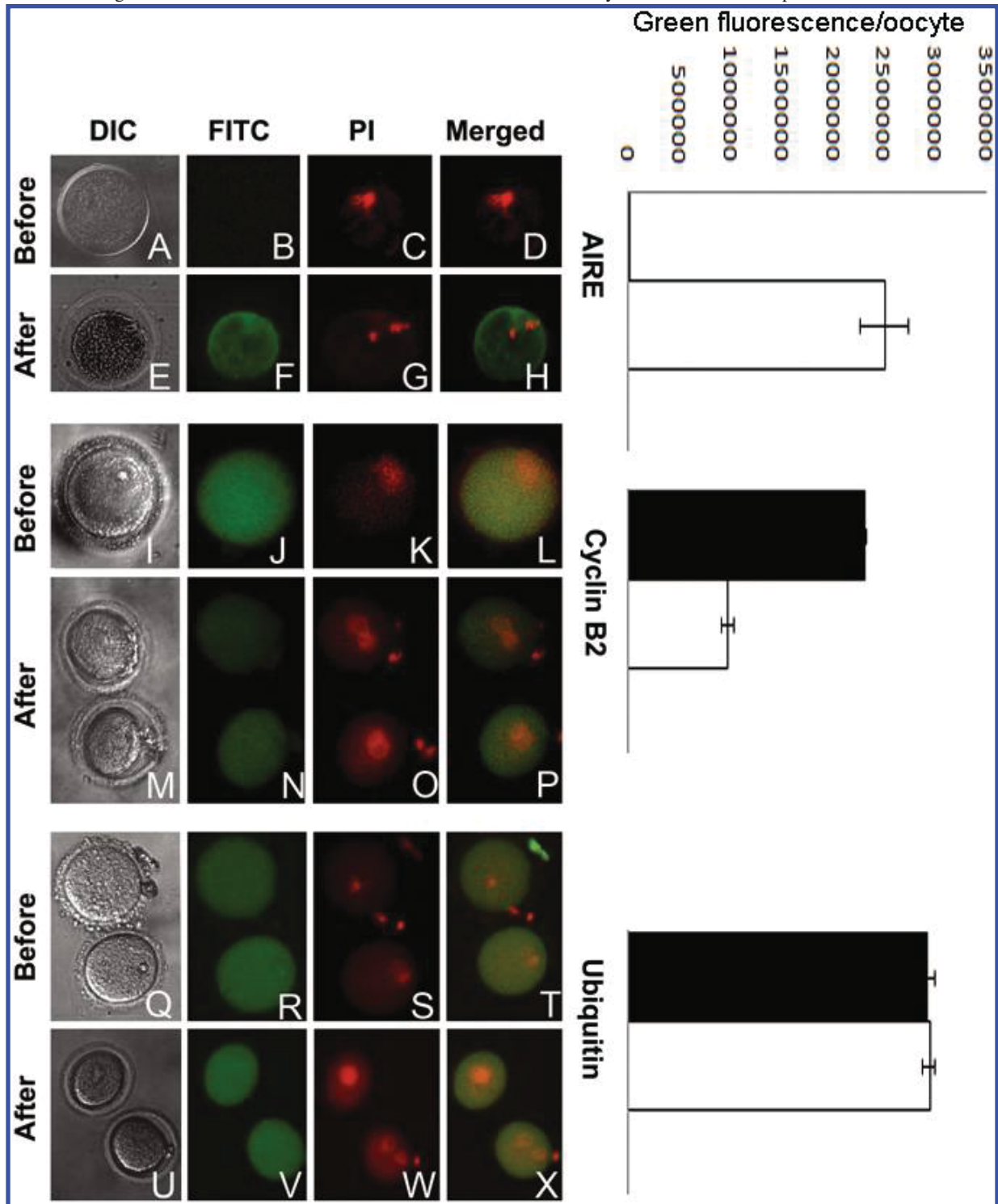
To further evaluate whether cyclin B2 degradation was indeed AIRE-dependent or merely correlative, we evaluated the degradation of goat testicular cyclin B2 in the presence of AIRE. Goat testicular extract showed a clear 48-kDa band that stained positively with cyclin B2 antibody (Fig. 9A, lane 2). This band was absent in cell lysate from untransformed BL21(DE3) (Fig. 9A, lane 3), which is referred to as BL21(DE3)-AIRE in subsequent sections of this paper. Goat testicular lysate showed a significant reduction in the levels of cyclin B2 within 60 min ($p < 0.01$) and 120 min ($p < 0.05$) of incubation with BL21 (DE3)-AIRE (Fig. 9A, lanes 4 and 7), which accounted for the intrinsic degradation of AIRE in our reactions. Furthermore, the addi-

tion of affinity-purified recombinant AIRE, along with BL21 (DE3)-AIRE, brought about a highly significant augmentation ($p < 0.0001$) in the degradation of cyclin B2 (Fig. 9A, lanes 5 and 8). The incubation of goat testicular lysate with bacterial lysate containing over-expressed AIRE (hereafter referred to as BL21(DE3)+AIRE) also brought about a highly significant ($p < 0.0001$) reduction in the levels of cyclin B2 within 1 h (Fig. 9A, lane 6) and 2 h (Fig. 9A, lane 9) of incubation compared with their respective controls, which were incubated with BL21(DE3)-AIRE (Fig. 9A, lanes 4 and 7). Cyclin B2 levels were reduced by 55% in reactions containing BL21 (DE3)-AIRE supplemented with rAIRE and by 86% in reactions containing BL21(DE3)+AIRE compared with the corresponding controls. The incubation of testis lysate with rAIRE for 3 h did not further enhance the degradation of cyclin B2 (Fig. 9B, lanes 2–5). MG-132 brought about a statistically significant reduction in the degradation of cyclin B2 (Fig. 9B, lanes 6 and 7).

Discussion

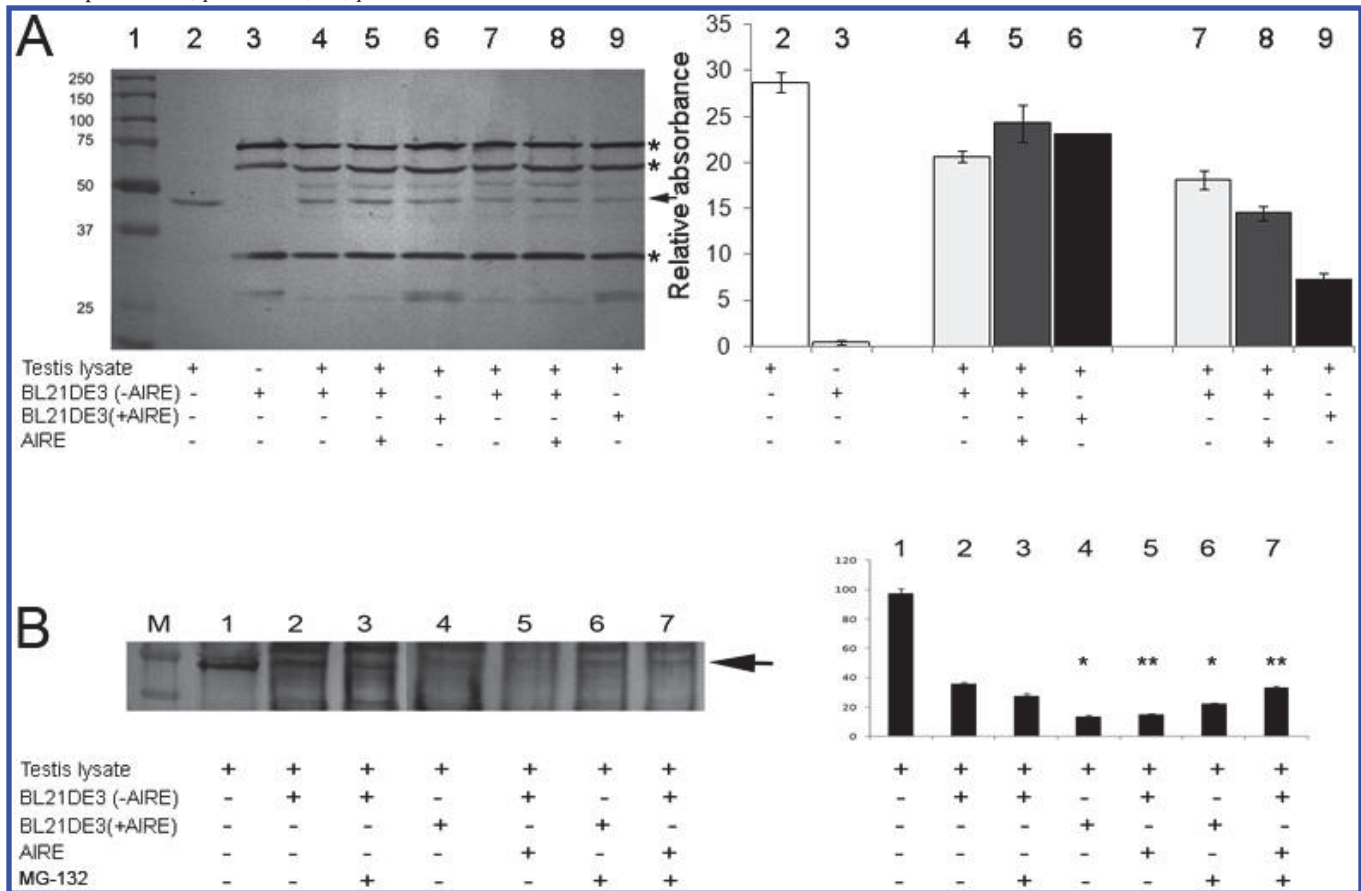
Beyond its well accepted function as a regulator of ectopic gene expression in thymus, *Aire*'s role in mouse testis—a tissue outside the immune system—is the focus of the present study. *Aire* demonstrates heavy expression profiles in adult testis (Halonen et al. 2001; Heino et al. 2000; Ruan et al. 1999). Deficiency of this gene product results in testicular failure, hypogonadism, oligomenorrhea, ovarian failure, and infertility (Maclaren et al. 2001; Meyer and Badenhop 2002). Using *Aire*-specific primers, we amplified a full-length *Aire* transcript, which showed 100% homology with AIRE variant 1 expressed in mouse thymus (AF079536). Immunoprecipitated AIRE from mouse testis lysates, as confirmed by peptide mass fingerprinting, authenticates the specificity of our laboratory-generated antibody. Our anti-AIRE antibody recognized recombinant AIRE and AIRE in thymus lysates (Fig. 3), further validating its specificity. On Western blots, AIRE could be detected in lysates of testis

Fig. 8. Immunocytochemical localization of AIRE, cyclin B2, and ubiquitin in mouse oocyte before and after fertilization in vivo. Confocal laser scan microscopy demonstrating the localization of AIRE (A–H), cyclin B2 (I–P), and ubiquitin (Q–X) in mouse oocytes and early zygotes. Bar diagrams on the right indicate the average of the total green channel signals per oocyte computed from nine individual oocytes for each of the experiments, and the error bars show the standard deviation within the observations. Empty bars represent observations from oocytes, whereas solid bars indicate those from early zygotes. Mouse oocyte stained negatively for AIRE before fertilization (B), but turned strongly positive for AIRE after fertilization in vivo (F). Oocytes stained strongly for cyclin B2 before fertilization (J), whereas there was a 60% reduction in cyclin B2 levels after fertilization (N). Ubiquitin levels remained unchanged in oocytes (R) and early embryos (V). Values presented in the histogram are the means \pm SD of the measurements from nine oocytes for each of the experiments.



Biochem. Cell Biol. Downloaded from www.nrcresearchpress.com by UNIV OF TEXAS AT ARLINGTON on 10/17/13
For personal use only.

Fig. 9. Cyclin B2 degradation assay. Goat testicular extract showed a 48-kDa band with cyclin B2 antibody (lane 2), which was absent in cell lysate from BL21(DE3)-AIRE (lane 3). Goat testicular lysates showed significant reductions in the levels of cyclin B2 within 60 min ($p < 0.01$) and 120 min ($p < 0.05$) of incubation with BL21 (DE3)-AIRE (lanes 4 and 7), compared with the levels of this protein in lane 2. This degradation accounted for the intrinsic degradation of AIRE in our reactions. The incubation of testicular lysate with recombinant AIRE and BL21 (DE3)-AIRE (lane 8) or BL21 (DE3)+AIRE (lane 9) for 2 h brought about significant AIRE degradation (lane 8). Cyclin B2 levels were reduced by 55% in reactions containing BL21 (DE3)-AIRE supplemented with rAIRE and by 86% in reactions containing BL21(DE3)+AIRE, compared with the corresponding controls. Incubation for 1 h under similar experimental conditions did not influence cyclin B2 degradation (lanes 5 and 6). Values presented in the histogram are the means \pm SD of the observations made in five replicates of the experiment. *, $p < 0.001$; **, $p < 0.0005$.



and spermatozoa harvested from various regions of the male reproductive tract. While salivary gland served as a negative control for AIRE, our failure to detect AIRE message (Fig. 1) or protein (Fig. 3B) in mouse bone marrow sharply contrasts with the previous observation of Halonen et al. (2001). However, it should be noted that these authors had also failed to detect AIRE message in bone marrow using RT-PCR, and had based their observation on immunohistochemistry using an anti-AIRE peptide antibody. Thus, we suspect an unexpected nonspecific cross reaction between their anti-AIRE antibody and some protein in bone marrow lysates.

The localization of AIRE protein was predominantly nuclear in immature testis, though the functional relevance of this observation is currently unclear. In adult testis sections, we could locate AIRE protein on spermatogonia and primary spermatocytes, which is consistent with the findings of Schaller et al. (2008), whereas AIRE protein on secondary spermatocytes and spermatozoa in various stages of development is novel. Confocal laser microscopy also revealed heavy localization of AIRE in the principal acrosomal segment (indicated with arrows in Fig. 5), which lost the pattern after the

acrosome reaction. The incubation of spermatozoa collected from cauda epididymidis with anti-AIRE antibody resulted in considerable sperm agglutination, confirming the assumption that the AIRE protein is located on accessible domains of membrane surfaces. The inhibition in sperm-oocyte interaction in the presence of anti-AIRE antibodies could be a result of sperm agglutination, but a more direct inhibition at the level of the binding of sperm to the oolemma cannot be ruled out. The *Aire*^{-/-} genotype is characterized by highly compromised fertility (Kuroda et al. 2005; Ramsey et al. 2002) associated with augmented peripheral T-cell proliferation and circulating autoantibodies (Ramsey et al. 2002). *Aire* has been argued to be involved in maintaining homeostatic regulation in the immune system rather than in T-cell education and development in the thymus; thus, we feel that the expression of *Aire* in mouse testicular germ cells would equip these cells with an intrinsic capacity to initiate local immune modulation and thereby escape autoimmune rejection of germ cells.

Because of the unorthodox position occupied by the AIRE protein on mouse spermatozoa, we evaluated the possibility

of AIRE being introduced into the oocyte by the spermatozoa during fertilization. Thus, mouse oocyte prior to sperm entry stained negatively for AIRE protein. However, after fertilization, the zygote stained positively for AIRE, indicating a possible introduction of AIRE into the oocyte by spermatozoa and (or) initiation of AIRE-expression in the oocyte after fertilization. However, this in vitro fertilization assay detected the appearance of AIRE within 30 min of the fusion of spermatozoa with the oocyte, which suggests the initial delivery of this protein into the oocyte during sperm-oocyte fusion rather than de novo gene expression in the early zygote. The correlation between the appearance of AIRE, the reduction in the levels of cyclin B2, and the abundance of ubiquitin in the zygote raised the possibility of AIRE-dependent cyclin B2 breakdown in the oocytes.

Since the evaluation of cyclin B2 degradation by AIRE-dependent mechanisms proved difficult in oocyte for technical reasons (results not presented), we decided to evaluate AIRE's degradation of cyclin B2 from goat testicular lysates. Affinity purified recombinant AIRE caused the degradation of cyclin B2 in the presence of BL21 (DE3)-AIRE (used as a source of E1/E2 ligases), establishing its direct involvement in cyclin B2 degradation. The correlation between the presence of AIRE and the degradation of cyclin B2, both in the zygote and in our in vitro assays, is relevant to the requirement of cyclin B2 breakdown for early embryo activation (Hyslop et al. 2004) and the possible function of AIRE as an E3 ubiquitin ligase (Uchida et al. 2004). Cyclin B2 is a meiotic checkpoint protein in oocytes (Uchida et al. 2004; Lemaître et al. 2002) and spermatogenic cells (Smirnova et al. 2006), the degradation of which has been argued to be mediated by ubiquitin-proteasome (Bodart et al. 1999). This study identifies cyclin B2 as a target protein that is specifically degraded through proteasomal pathways in an AIRE-dependent fashion, and renders novel insight into the functions of AIRE as a multifunctional protein.

Acknowledgements

This work was supported by grants from Department of Biotechnology (BT/PR1316/Med/09/212/98) and Department of Science and Technology (SP/SO/B47/2000). M. Brahmaraju received a Senior Research fellowship (9/716(58)/2002-EMR-1) from Council of Scientific and Industrial Research, New Delhi. V. Jiji and Sandhya C. Nair provided technical help in confocal imaging and P. Manoj in DNA sequencing.

References

- Anderson, M.S., Venanzi, E.S., Klein, L., Chen, Z., Berzins, S.P., Turley, S.J., et al. 2002. Projection of an immunological self shadow within the thymus by the aire protein. *Science*, **298**(5597): 1395–1401. doi:10.1126/science.1075958. PMID:12376594.
- Bodart, J.F., Bechard, D., Bertout, M., Gannon, J., Rousseau, A., Vilain, J.P., and Flament, S. 1999. Activation of *Xenopus* eggs by the kinase inhibitor 6-DMAP suggests a differential regulation of cyclin B and p39(mos) proteolysis. *Exp. Cell Res.* **253**(2): 413–421. doi:10.1006/excr.1999.4662. PMID:10585264.
- Duesbery, N.S., and Vande Woude, G.F. 2002. Developmental biology: an arresting activity. *Nature*, **416**(6883): 804–805. doi:10.1038/416804a. PMID:11976667.
- Ferguson, B.J., Alexander, C., Rossi, S.W., Liiv, I., Rebane, A., Worth, C.L., et al. 2008. AIRE's CARD revealed, a new structure for central tolerance provokes transcriptional plasticity. *J. Biol. Chem.* **283**(3): 1723–1731. doi:10.1074/jbc.M707211200. PMID:17974569.
- Halonen, M., Pelto-Huikko, M., Eskelin, P., Peltonen, L., Ulmanen, I., and Kolmer, M. 2001. Subcellular location and expression pattern of autoimmune regulator (Aire), the mouse orthologue for human gene defective in autoimmune polyendocrinopathy candidiasis ectodermal dystrophy (APECED). *J. Histochem. Cytochem.* **49**(2): 197–208. doi:10.1177/002215540104900207. PMID:11156688.
- Heino, M., Peterson, P., Sillanpaa, N., Guerin, S., Wu, L., Anderson, G., et al. 2000. RNA and protein expression of the murine autoimmune regulator gene (Aire) in normal, RelB-deficient and in NOD mouse. *Eur. J. Immunol.* **30**(7): 1884–1893. doi:10.1002/1521-4141(200007)30:7<1884::AID-IMMU1884>3.0.CO;2-P. PMID:10940877.
- Hubert, F.X., Kinkel, S.A., Webster, K.E., Cannon, P., Crewther, P. E., Proeitto, A.I., et al. 2008. A specific anti-*aire* antibody reveals *aire* expression is restricted to medullary thymic epithelial cells and not expressed in periphery. *J. Immunol.* **180**(6): 3824–3832. PMID:18322189.
- Hyslop, L.A., Nixon, V.L., Levasseur, M., Chapman, F., Chiba, K., McDougall, A., et al. 2004. Ca(2+)-promoted cyclin B1 degradation in mouse oocytes requires the establishment of a metaphase arrest. *Dev. Biol.* **269**(1): 206–219. doi:10.1016/j.ydbio.2004.01.030. PMID:15081368.
- Kumar, G.P., Laloraya, M., Agrawal, P., and Laloraya, M.M. 1990. The involvement of surface sugars of mammalian spermatozoa in epididymal maturation and in vitro sperm-zona recognition. *Andrologia*, **22**(2): 184–194. doi:10.1111/j.1439-0272.1990.tb01964.x. PMID:2264622.
- Kumar, P.G., Laloraya, M., and Laloraya, M.M. 1991. Superoxide radical level and superoxide dismutase activity changes in maturing mammalian spermatozoa. *Andrologia*, **23**(2): 171–175. PMID:1659251.
- Kumar, P.G., Laloraya, M., Wang, C.Y., Ruan, Q.G., Davoodi-Semiromi, A., Kao, K.J., and She, J.X. 2001. The autoimmune regulator (AIRE) is a DNA-binding protein. *J. Biol. Chem.* **276**(44): 41357–41364. doi:10.1074/jbc.M104898200. PMID:11533054.
- Kumar, P.G., Laloraya, M., and She, J.X. 2002. Population genetics and functions of the autoimmune regulator (AIRE). *Endocrinol. Metab. Clin. North Am.* **31**(2): 321–338, vi. [vi.] doi:10.1016/S0889-8529(01)00011-1. PMID:12092453.
- Kuroda, N., Mitani, T., Takeda, N., Ishimaru, N., Arakaki, R., Hayashi, Y., et al. 2005. Development of autoimmunity against transcriptionally unrepressed target antigen in the thymus of Aire-deficient mice. *J. Immunol.* **174**(4): 1862–1870. PMID:15699112.
- Lemaître, J.M., Bocquet, S., and Méchali, M. 2002. Competence to replicate in the unfertilized egg is conferred by Cdc6 during meiotic maturation. *Nature*, **419**(6908): 718–722. doi:10.1038/nature01046. PMID:12384698.
- Liiv, I., Rebane, A., Org, T., Saare, M., Maslovskaja, J., Kisand, K., et al. 2008. DNA-PK contributes to the phosphorylation of AIRE: importance in transcriptional activity. *Biochim. Biophys. Acta*, **1783**(1): 74–83. doi:10.1016/j.bbamcr.2007.09.003. PMID:17997173.
- Maclaren, N., Chen, Q.Y., Kukreja, A., Marker, J., Zhang, C.H., and Sun, Z.S. 2001. Autoimmune hypogonadism as part of an autoimmune polyglandular syndrome. *J. Soc. Gynecol. Investig.* **8**(1 Suppl. Proceedings): S52–S54. doi:10.1016/S1071-5576(00)00109-X. PMID:11223374.
- Mahaffey, D.T., Yoo, Y., and Rechsteiner, M. 1995. Ubiquitination of

- full-length cyclin. *FEBS Lett.* **370**(1–2): 109–112. doi:10.1016/0014-5793(95)00799-F. PMID:7649287.
- Meyer, G., and Badenhop, K. 2002. Autoimmune regulator (AIRE) gene on chromosome 21: implications for autoimmune polyendocrinopathy-candidiasis-ectodermal dystrophy (APECED) any more common manifestations of endocrine autoimmunity. *J. Endocrinol. Invest.* **25**(9): 804–811. PMID:12398240.
- Mittaz, L., Rossier, C., Heino, M., Peterson, P., Krohn, K.J., Gos, A., et al. 1999. Isolation and characterization of the mouse Aire gene. *Biochem. Biophys. Res. Commun.* **255**(2): 483–490. doi:10.1006/bbrc.1999.0223. PMID:10049735.
- Mizoguchi, H., and Dukelow, W.R. 1980. Effect of timing of hCG injection on fertilization in superovulated hamsters. *Biol. Reprod.* **23**(1): 237–241. doi:10.1095/biolreprod23.1.237. PMID:7417666.
- Nagamine, K., Peterson, P., Scott, H.S., Kudoh, J., Minoshima, S., Heino, M., et al. 1997. Positional cloning of the APECED gene. *Nat. Genet.* **17**(4): 393–398. doi:10.1038/ng1297-393. PMID:9398839.
- Ooi, S.K., Qiu, C., Bernstein, E., Li, K., Jia, D., Yang, Z., et al. 2007. DNMT3L connects unmethylated lysine 4 of histone H3 to de novo methylation of DNA. *Nature*, **448**(7154): 714–717. doi:10.1038/nature05987. PMID:17687327.
- Oven, I., Brdickova, N., Kohoutek, J., Vaupotic, T., Narat, M., and Peterlin, B.M. 2007. AIRE recruits P-TEFb for transcriptional elongation of target genes in medullary thymic epithelial cells. *Mol. Cell. Biol.* **27**(24): 8815–8823. doi:10.1128/MCB.01085-07. PMID:17938200.
- Peter, M., Castro, A., Lorca, T., Le Peuch, C., Magnaghi-Jaulin, L., Dorée, M., and Labbé, J.C. 2001. The APC is dispensable for first meiotic anaphase in *Xenopus* oocytes. *Nat. Cell Biol.* **3**(1): 83–87. doi:10.1038/35050607. PMID:11146630.
- Puissant, B. 2004. Fonction thymique et auto-immunité. *Rev. Med. Interne*, **25**(8): 562–572. doi:10.1016/j.revmed.2003.12.017. PMID:15276288.
- Ramsey, C., Winqvist, O., Puhakka, L., Halonen, M., Moro, A., Kampe, O., et al. 2002. Aire deficient mice develop multiple features of APECED phenotype and show altered immune response. *Hum. Mol. Genet.* **11**(4): 397–409. doi:10.1093/hmg/11.4.397. PMID:11854172.
- Ruan, Q.G., Wang, C.Y., Shi, J.D., and She, J.X. 1999. Expression and alternative splicing of the mouse autoimmune regulator gene (Aire). *J. Autoimmun.* **13**(3): 307–313. doi:10.1006/jaut.1999.0326. PMID:10550218.
- Schaller, C.E., Wang, C.L., Beck-Engeser, G., Goss, L., Scott, H.S., Anderson, M.S., and Wabl, M. 2008. Expression of Aire and the early wave of apoptosis in spermatogenesis. *J. Immunol.* **180**(3): 1338–1343. PMID:18209027.
- Smirnova, N.A., Romanienko, P.J., Khil, P.P., and Camerini-Otero, R.D. 2006. Gene expression profiles of Spo11–/– mouse testes with spermatocytes arrested in meiotic prophase I. *Reproduction*, **132**(1): 67–77. doi:10.1530/rep.1.00997. PMID:16816334.
- Uchida, D., Hatakeyama, S., Matsushima, A., Han, H., Ishido, S., Hotta, H., et al. 2004. AIRE functions as an E3 ubiquitin ligase. *J. Exp. Med.* **199**(2): 167–172. doi:10.1084/jem.20031291. PMID:14734522.
- Yu, Q., and Wu, J. 2008. Involvement of cyclins in mammalian spermatogenesis. *Mol. Cell. Biochem.* **315**(1–2): 17–24. doi:10.1007/s11010-008-9783-8. PMID:18470654.
- Zhao, Q., Rank, G., Tan, Y.T., Li, H., Moritz, R.L., Simpson, R.J., et al. 2009. PRMT5-mediated methylation of histone H4R3 recruits DNMT3A, coupling histone and DNA methylation in gene silencing. *Nat. Struct. Mol. Biol.* **16**(3): 304–311. doi:10.1038/nsmb.1568. PMID:19234465.
- Zuklys, S., Balciunaite, G., Agarwal, A., Fasler-Kan, E., Palmer, E., and Hollander, G.A. 2000. Normal thymic architecture and negative selection are associated with Aire expression, the gene defective in the autoimmune-polyendocrinopathy-candidiasis-ectodermal dystrophy (APECED). *J. Immunol.* **165**(4): 1976–1983. PMID:10925280.